Molecular Cell
Article

The Nonspecific Lethal Complex Is a Transcriptional Regulator in *Drosophila*

Sunil Jayaramaiah Raja,[1,2,5] Iryna Charapitsa,[1,2,5] Thomas Conrad,[1,2] Juan M. Vaquerizas,[3] Philipp Gebhardt,[1] Herbert Holz,[1,2] Jan Kadlec,[4] Sven Fraterman,[1] Nicholas M. Luscombe,[1,3] and Asifa Akhtar[1,2,*]
[1]Genome Biology Unit, European Molecular Biology Laboratory, Meyerhofstrasse 1, 69117 Heidelberg, Germany
[2]Max Planck Institute of Immunobiology, Stubeweg 51, D-79108 Freiburg, Germany
[3]European Molecular Biology Laboratory European Bioinformatics Institute, Wellcome Trust Genome Campus, Cambridge CB10 1SD, UK
[4]European Molecular Biology Laboratory Grenoble, 6, rue Jules Horowitz, BP 181, 38042 Grenoble Cedex 9, France
[5]These authors contributed equally to this work
*Correspondence: akhtar@immunbio.mpg.de
DOI 10.1016/j.molcel.2010.05.021

SUMMARY

Here, we report the biochemical characterization of the nonspecific lethal (NSL) complex (NSL1, NSL2, NSL3, MCRS2, MBD-R2, and WDS) that associates with the histone acetyltransferase MOF in both *Drosophila* and mammals. Chromatin immunoprecipitation-Seq analysis revealed association of NSL1 and MCRS2 with the promoter regions of more than 4000 target genes, 70% of these being actively transcribed. This binding is functional, as depletion of MCRS2, MBD-R2, and NSL3 severely affects gene expression genome wide. The NSL complex members bind to their target promoters independently of MOF. However, depletion of MCRS2 affects MOF recruitment to promoters. NSL complex stability is interdependent and relies mainly on the presence of NSL1 and MCRS2. Tethering of NSL3 to a heterologous promoter leads to robust transcription activation and is sensitive to the levels of NSL1, MCRS2, and MOF. Taken together, we conclude that the NSL complex acts as a major transcriptional regulator in *Drosophila*.

INTRODUCTION

Eukaryotic genes that encode messenger RNAs are subject to primary regulation at the level of transcription. A series of distinct phases occur at the onset of transcription of these RNAs, beginning with the binding of activators upstream of the core promoter, followed by the recruitment of adaptor complexes such as SAGA or mediator. In turn those adaptor complexes facilitate the binding of general transcription factors (GTFs) and RNA polymerase II and initiate transcription (Thomas and Chiang, 2006). To better understand the mechanism of transcription initiation, characterization of yet-unidentified promoter-bound proteins is essential.

Transcription initiation in eukaryotes involves dynamic changes in chromatin structure that permit assembly of the transcription machinery at a gene promoter (Lemon and Tjian, 2000; Orphanides and Reinberg, 2000). The fundamental structural unit of chromatin is the nucleosome, which contains 146 bp of DNA wrapped around a histone octamer composed of two copies each of histones H2A, H2B, H3, and H4. Histones in a nucleosomal context are subject to a variety of posttranslational modifications, such as acetylation, methylation, phosphorylation, ribosylation, ubiquitinylation, etc. A number of well-conserved enzymes carry out these modifications (for review, see Kouzarides, 2007).

Males absent on first (MOF) is a histone H4 lysine 16 specific acetyltransferase in both *Drosophila* and mammals (Hilfiker et al., 1997; Mendjan et al., 2006; Smith et al., 2000; Taipale et al., 2005). In *Drosophila*, MOF is well known for its role in dosage compensation of the male X chromosome in the context of the male specific lethal (MSL) complex (Akhtar and Becker, 2000; Hilfiker et al., 1997; Kind et al., 2008; Smith et al., 2000, 2001). Genome-wide high-resolution binding profiles of MOF along with MSL1 and MSL3 have shown that MSLs are enriched primarily toward the 3′ end of X-linked genes. In contrast, MOF also binds to promoter proximal regions of the same genes as well as to a large number of autosomal promoters, independently of the other MSL complex members (Alekseyenko et al., 2006, 2008; Gilfillan et al., 2006; Kind et al., 2008; Legube et al., 2006). However, it remained unclear whether MOF binds to promoters alone or whether it is associated with additional proteins.

Our previous studies have shown that MOF associates not only with the MSL complex members, but also with a number of uncharacterized proteins such as CG4699 (NSL1), CG18041 (NSL2), CG8233 (NSL3), CG1135 (MCRS2), and CG10042 (MBD-R2). These proteins were named as nonspecific lethal (NSL) proteins since disruption of the respective genes by *P*-element insertions in *Drosophila* is early larval lethal in both sexes (Mendjan et al., 2006). However, it remained unknown whether there was any functional link between these proteins and MOF.

To gain further insight, in the present study, we performed the purification and functional characterization of TAP-tagged MCRS2 and TAP-HA-FLAG-tagged NSL1. We find NSL1, NSL2, NSL3, MCRS2, MBD-R2, WDS, and MOF consistently purified as a complex, which we name the NSL complex.

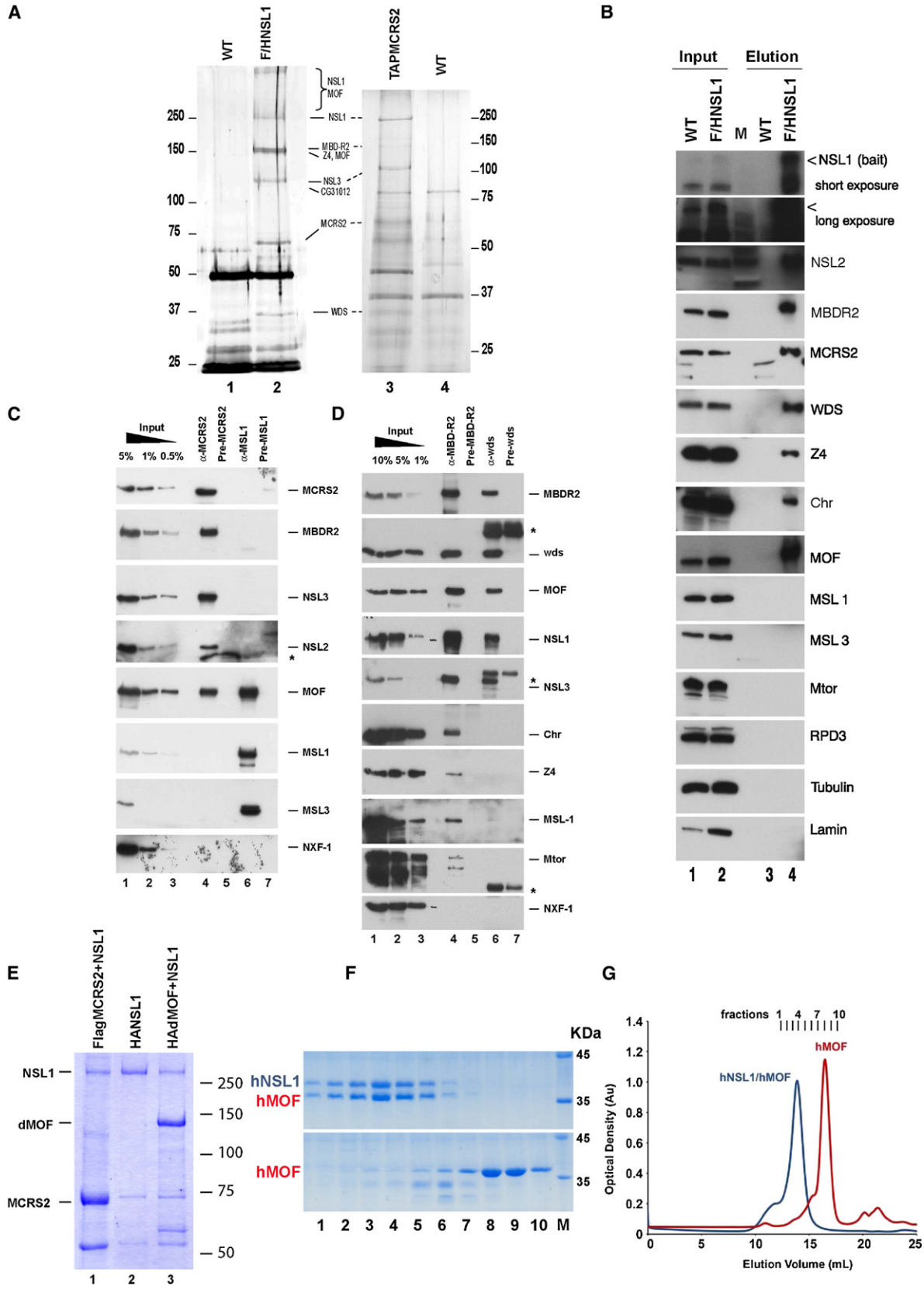
A
WT
F/HNSL1
TAPMCRS2
WT
NSL1
MOF
NSL1
MBD-R2
Z4, MOF
NSL3
CG31012
MCRS2
WDS
250
150
100
75
50
37
25
1
2
3
4
B
Input
Elution
WT
F/HNSL1
M
WT
F/HNSL1
NSL1 (bait)
short exposure
long exposure
NSL2
MBDR2
MCRS2
WDS
Z4
Chr
MOF
MSL 1
MSL 3
Mtor
RPD3
Tubulin
Lamin
1 2 3 4
C
Input
5% 1% 0.5%
α-MCRS2
Pre-MCRS2
α-MSL1
Pre-MSL1
MCRS2
MBDR2
NSL3
NSL2
MOF
MSL1
MSL3
NXF-1
1 2 3 4 5 6 7
D
Input
10% 5% 1%
α-MBD-R2
Pre-MBD-R2
α-wds
Pre-wds
MBDR2
wds
MOF
NSL1
NSL3
Chr
Z4
MSL-1
Mtor
NXF-1
1 2 3 4 5 6 7
E
FlagMCRS2+NSL1
HANSL1
HAdMOF+NSL1
NSL1
dMOF
MCRS2
250
150
100
75
50
1
2
3
F
KDa
hNSL1
hMOF
hMOF
45
35
45
35
1 2 3 4 5 6 7 8 9 10 M
G
fractions 1 4 7 10
hMOF
hNSL1/hMOF
Optical Density (Au)
1.4
1.2
1.0
0.8
0.6
0.4
0.2
0
0 5 10 15 20 25
Elution Volume (mL)

Interestingly, members of the NSL complex bind to MOF target promoters on the X chromosome and autosomes in both sexes. Chromatin immunoprecipitation (ChIP)-Seq profiling for NSL1 and MCRS2 reveals that these proteins together bind to the promoters of more than 4000 target genes. The NSL complex members bind to their target promoters independently of MOF. However, MOF targeting to promoters is NSL complex dependent, showing a hierarchy of recruitment. Furthermore, upon depletion of NSL1, NSL3, or MCRS2, the stability of the NSL complex is compromised. MCRS2, MBD-R2, and NSL3 are important regulators of gene expression, as their depletion severely affects the mRNA levels of most of the NSL target genes in a genome-wide manner. Our data suggest that reduction in transcript levels is the result of impaired transcription initiation, since it correlates with reduced levels of RNA polymerase II at gene promoters. In addition, we show that tethering NSL3 to a heterologous promoter activates transcription, and that the NSL complex members as well as MOF modulate this activity. These results suggest a cooperative interaction between the NSL complex members and MOF. Taken together, we identify the NSL complex as an evolutionarily conserved complex, which acts as a major transcriptional regulator in *Drosophila*.

RESULTS

Biochemical Purification of the NSL Complex

Our previous copurification of MOF interacting proteins identified a set of proteins of unknown function (Mendjan et al., 2006). To gain further insight into the nature of these interactions, we generated stable Schneider (SL-2) cell lines expressing two of the uncharacterized proteins—TAP-tagged MCRS2 and TAP-HA-FLAG-tagged NSL1. Nuclear extracts were prepared from cell lines that express tagged proteins as well as from wild-type cells for mock purification. The quality of the affinity-purified material was analyzed by SDS-PAGE followed by silver staining (Figure 1A). Matrix-assisted laser desorption/ionization time of flight, nanoelectrospray, liquid chromatography-tandem mass spectrometry, as well as western blot analysis identified the following proteins consistently purifying with either NSL1 or MCRS2: NSL1, NSL2, NSL3, MCRS2, MBD-R2, WDS, and MOF in addition to a number of other proteins (Figure 1A; Table S1, available online).

The *nsl1* gene is located on chromosome 3R and encodes a protein of 1550 aa which contains a MOF interacting PEHE domain at its C terminus. The *nsl2* gene is located on chromosome 3R and encodes a protein of 484 aa that contains two C/H-rich domains. The *nsl3* gene is located on chromosome 2R and encodes three splice variant proteins of 1001 aa, 1066 aa, and 934 aa, all containing a α/β hydrolase domain. The *mcrs2* gene is located on chromosome 3L and encodes a protein of 578 aa containing a ForkHead-Associated domain (FHA) at its C terminus. The *mbd-r2* gene is located on chromosome 3R and encodes two splice variants: one variant of 1169 aa containing a Tudor, MBD, ZnF and a PHD finger domain and a second variant of 1081 aa without the Tudor domain (Hendrich and Tweedie, 2003).

None of these proteins were found in the control mock purification from the wild-type SL-2 cell line, thus validating the purification assay. The interactions were further confirmed by western blot analysis of the eluted fractions (Figure 1B). Interestingly, apart from MOF, none of the other MSL complex proteins copurified with MCRS2 or NSL1. These results, as well as coimmunoprecipitation experiments with WDS, MBD-R2, MCRS2, and MSL1-specific antibodies revealed that the interaction between these proteins and MOF was specific and distinct from the previously characterized MSL complex (Figures 1C and 1D). Among the proteins tested in coimmunoprecipitation experiments only MBD-R2 revealed a substoichiometric interaction with MSL1. We termed this copurified complex containing NSL1, NSL2, NSL3, MCRS2, MBD-R2, WDS, and MOF as the NSL complex. NSL complex elutions were also tested for histone acetyltransferase (HAT) activity. Indeed, we detect an enrichment of histone H4 directed HAT activity in these fractions (Figures S1A and S1B).

NSL1 Directly Interacts with MCRS2 and MOF

In order to dissect the interactions between the NSL proteins, expression constructs with tagged (FLAG or HA) as well as untagged NSL1, MCRS2, and MOF were expressed in the baculovirus expression system (Figure 1E; data not shown). Copurification of these proteins revealed a stable interaction of NSL1 with MCRS2 and MOF (Figure 1E, lanes 1–3). These results showed that the interaction between NSL1-MCRS2 and NSL1-MOF is direct and can occur in the absence of other NSL

Figure 1. Purification of the NSL1 and MCRS2 Complexes

(A) Silver staining of copurified proteins from Schneider SL-2 cells stably expressing TAP-FLAG-HA-NSL1 (lanes 1 and 2) and TAP-MCRS2 (lanes 3 and 4). WT indicates corresponding mock purifications from wild-type SL-2 cells. From each cell line 1.5 ml of nuclear extract with a protein concentration of 6μg/μl was used, and 50% of the purified eluted material was loaded on a gel; the rest of the material was used for subsequent mass spectrometry analysis. The bracket indicates an additional area on the gel where NSL1 and MOF peptides were identified upon band excision by mass spectrometry analysis.

(B) Western blot analysis of the TAP-FLAG-HA-NSL1 (TFH-NSL1) purification for NSL proteins. NSL1, NSL2, MCRS2, MBD-R2, WDS, Z4, Chromator, and MOF were detected in the final eluate, but not MSL1 and MSL3. Tubulin and lamin served as negative controls. The open arrow indicates the NSL1 bait. Long exposure is shown for detection of NSL1 in input lanes.

(C) Immunoprecipitation from *Drosophila* embryo nuclear extract with α-MCRS2 or α-MSL1 antisera. The blot was probed with various antibodies as indicated. Asterisks represent the IgG band.

(D) Same as in (C), except immunoprecipitations were performed with α-MBDR2 or α-WDS antibodies.

(E) Reconstitution of NSL interactions using baculovirus-expressed proteins. Interaction of NSL1 with MCRS2 (lane 1) and *Drosophila* MOF (dMOF, lane 3) upon incubation of protein extracts. Purification of HA-tagged NSL1 alone (lane 2). After purification via the corresponding tag, proteins were run on a SDS-PAGE and the gel stained with Coomassie blue.

(F) Fractions 1 to 10 of the hNSL1 (aa 883–1105)/hMOF (aa 174–458) (top) and hMOF (aa 174–458) (bottom) Superdex 200 gel filtration profiles. Fractions were run on a SDS-PAGE and the gel stained with Coomassie blue.

(G) Superdex 200 gel filtration elution profiles of hNSL1 (aa 883–1105)/hMOF (aa 174–458) in blue and of hMOF (174-458) in red.

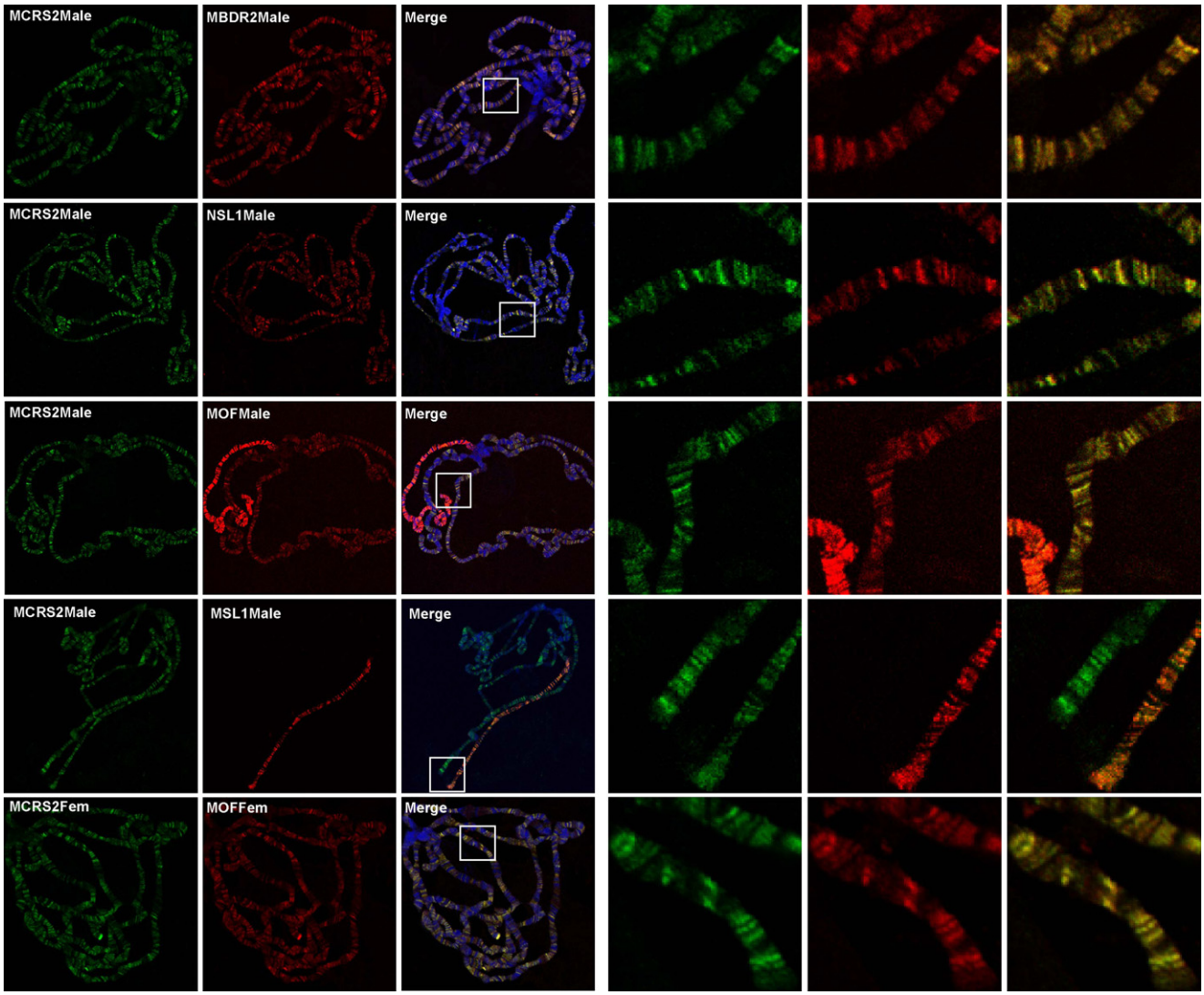

Figure 2. MCRS2, MBD-R2, NSL1, and MOF Colocalize Globally on Wild-Type Male and Female *Drosophila* Third Instar Larval Polytene Chromosomes

Coimmonufluroscence staining of MCRS2 (green) with MBD-R2, NSL1, MOF, and MSL1 (red); DNA counterstained by Hoechst. As a control of binding specificity, coimmunostaining of MCRS2 and MSL1 is shown. White boxes indicate the zoomed area in the right panels showing the extent of colocalization.

complex members. We further characterized the interaction for the mammalian orthologs hMOF and hNSL1 and could observe that the HAT domain of hMOF (aa 174–458) and the C-terminal domain of hNSL1 (aa 883–1105) were sufficient for interaction. Furthermore, gel filtration as well as multiangle laser light scattering (MALLS) analyses revealed that this interaction was based on a stoichiometry of 1:1 between the two proteins (Figures 1F and 1G; Figure S1C). These results further demonstrate the high degree of evolutionary conservation between NSL1 and MOF interaction across species.

The NSL Complex Members Are Localized on MOF Target Promoters

The biochemical association of NSL proteins with MOF prompted us to address whether these proteins are chromatin bound in vivo. We therefore performed immunofluoresence staining of *Drosophila* third instar larval male and female polytene chromosomes using antibodies against MCRS2, NSL1, MBD-R2, and MOF. All four proteins showed extensive genome-wide colocalization with each other as well as with MOF on interbands of the polytene chromosome squash preparations in both sexes (Figure 2; Figure S2A, available online).

To gain more detailed insight as to where chromatin binding was occurring, ChIP assay was performed on wild-type male salivary glands using antibodies against MCRS2, MBD-R2, NSL1, and MOF; corresponding preimmune sera were used as negative controls. ChIP samples were analyzed using quantitative real-time PCR (qPCR). Seven genes, which were recently identified as MOF target genes either on X chromosomal (*CG6506*, *CG4406*, *Dspt6*, and *Rb*) or autosomal (*Sec5*,

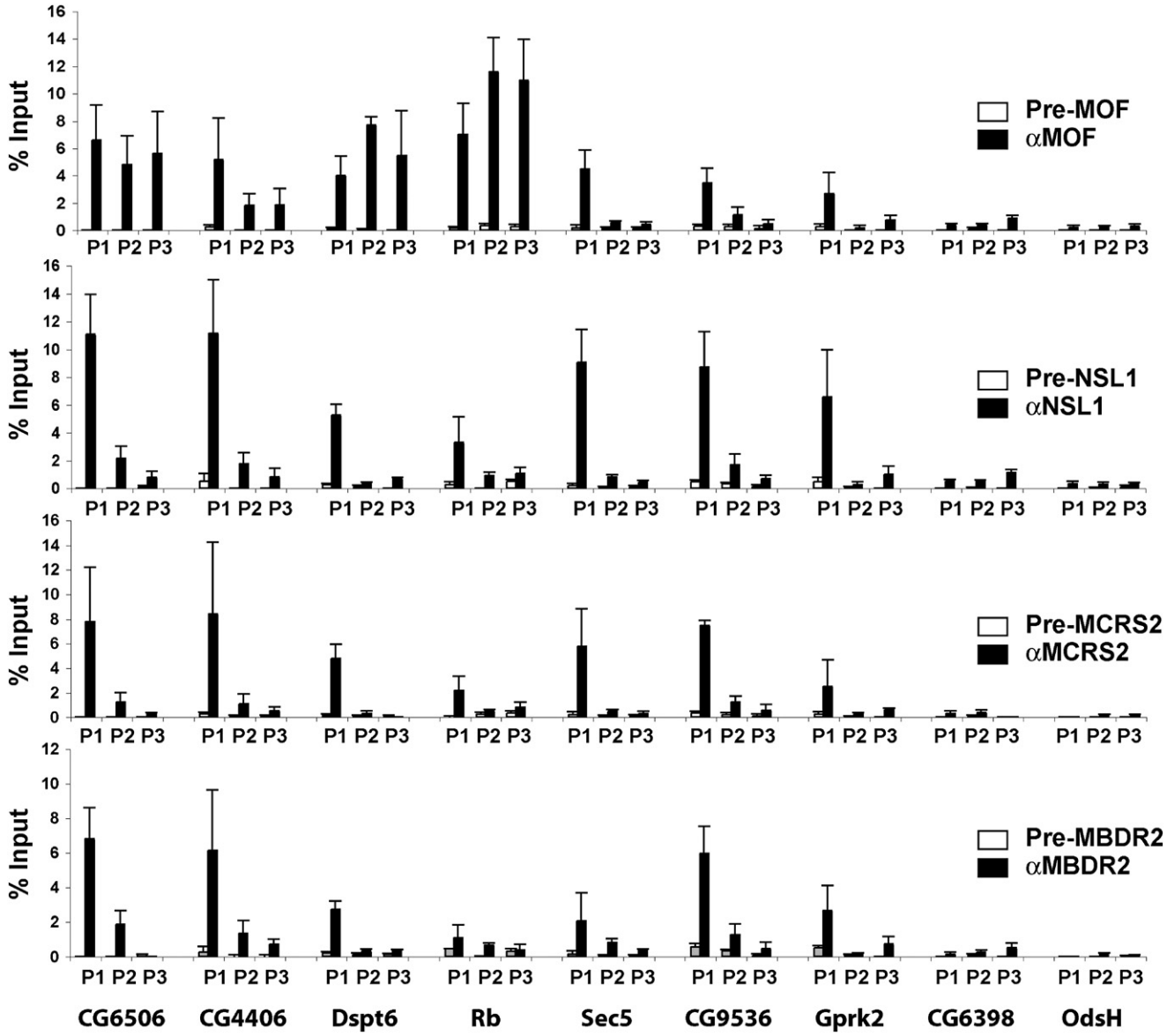

Figure 3. NSL1, MCRS2, and MBD-R2 Bind to the Promoters of X Chromosomal and Autosomal Genes

ChIP analysis from larval male salivary glands using antibodies against MOF, NSL1, MCRS2, and MBD-R2. Respective preimmune sera were used as negative controls. Immunoprecipitated DNA was amplified by qPCR with primer sets indicated in the Supplemental Experimental Procedures. Six X-linked genes (*CG6506*, *CG4406*, *Dspt6*, *Rb*, *CG6398*, and *OdsH*) and three autosomal genes (*Sec5*, *CG9536*, and *Gprk2*) were evaluated using primers positioned at the promoter (P1), middle (P2), and end (P3) of the coding sequence. Percentage input is determined as the amount of immunoprecipitated DNA relative to input DNA. Error bars represent standard deviation (StDev) of five independent experiments.

CG9536, and *Gprk2*) locations (Kind et al., 2008), were tested for NSL binding. Two MOF nontarget genes (*CG6398* and *OdsH*) were used as negative controls. Distribution on each gene was analyzed using primers located toward the promoter (P1), middle (P2), and the end of the coding region (P3) as indicated in Figure 3 (also see Experimental Procedures). Consistent with previous studies (Kind et al., 2008), MOF showed binding to the promoter regions of autosomal genes, whereas on X chromosomal targets, binding is also distributed along the transcribed regions (compare Figure 3, X targets versus autosomal targets). Interestingly, we found that NSL1, MCRS2, and MBD-R2 are enriched on promoter proximal regions of X chromosomal as well as autosomal MOF target genes (Figure 3). To further address whether this binding pattern is specific to male salivary glands, we performed ChIP from female salivary glands, SL-2 cells, as well as from whole larvae, which showed the same results (Figures S2B–S2D). Furthermore, to get a global perspective, ChIP followed by Solexa deep sequencing analysis revealed that clusters of MCRS2 and NSL1 highly coincide on promoters, suggesting that these proteins act in a complex also in the chromatin

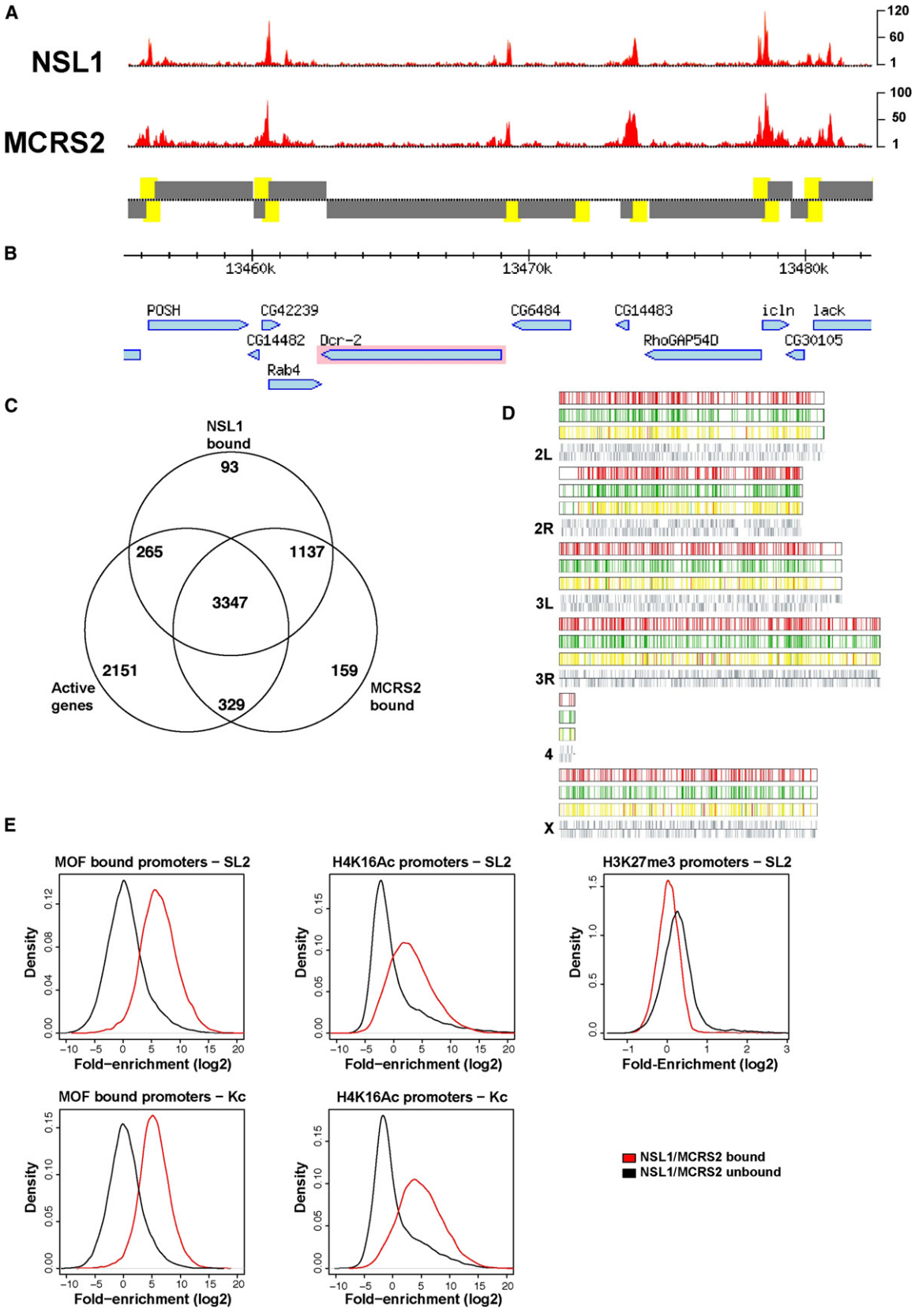
A
NSL1
MCRS2
120
60
1
100
50
1
B
13460k
13470k
13480k
POSH
CG42239
CG14482
Dcr-2
Rab4
CG6484
CG14483
RhoGAP54D
icln
lack
CG30105
C
NSL1 bound
93
265
1137
3347
2151
159
329
Active genes
MCRS2 bound
D
2L
2R
3L
3R
4
X
E
MOF bound promoters – SL2
H4K16Ac promoters – SL2
H3K27me3 promoters – SL2
MOF bound promoters – Kc
H4K16Ac promoters – Kc
Density
Fold–enrichment (log2)
Fold-Enrichment (log2)
NSL1/MCRS2 bound
NSL1/MCRS2 unbound

context (Figures 4A, 4B, and 4D; Figure S3A, available online). Over 4000 promoters were bound by NSL1 and MCRS2, ~70% of these corresponding to active genes ($p < 2.2e-16$; Fisher's exact test; Figure 4C). Correlation with the 5′ end of primary transcripts confirmed that NSL1 and MCRS2 binding peaks near transcription start sites. The most frequent distance to the nearest cluster of NSL1 and MCRS2 binding is −45 bp upstream and +2 bp downstream from the transcription start sites, respectively (Figures S3B and S3C). Furthermore, H4K16Ac and MOF binding are enriched at promoters of NSL-bound genes when compared with promoters of genes not bound by MCRS2 and NSL1 (Figure 4E). This happens for both SL-2 and Kc cells ($p < 2.2e-16$ for all cases; t test). In contrast, H3K27me3, a mark enriched on inactive genes (Schwartz et al., 2006), is depleted on promoters bound by MCRS2 and NSL1 ($p < 2.2e-16$; t test). Taken together, the above results reveal the NSL complex as a promoter-bound complex in *Drosophila*.

NSL1 and MCRS2 Are Required for the Stability of the NSL Complex

P-element insertions in *MBD-R2*, *MCRS2*, and *NSL3* lead to early larval lethality in both sexes (see Supplemental Experimental Procedures available online). Therefore, to analyze the functional significance of the NSL complex, we performed tissue-specific RNAi-mediated knockdown in *Drosophila* using the Gal4-upstream activating sequence (UAS) system (Brand and Perrimon, 1993). RNAi-mediated knockdown of MBD-R2, MCRS2, and NSL3 in eye imaginal discs using an *eyeless*-Gal4 driver resulted in a reduced, rough eye phenotype signifying that these proteins are important for development (Figure S4, available online).

To further examine the fate of the NSL complex components upon depletion of individual proteins of the complex, we chose to knockdown MCRS2, MBD-R2, and NSL3 in the salivary glands using *patched*-Gal4,UAS-EGFP/+;UAS-RNAi/+, where EGFP positively marks the knockdown cells. Upon depletion of these proteins, the development of salivary glands is impaired, as observed by reduced gland size (data not shown). Interestingly, depletion of MCRS2 led to a severe reduction of nuclear NSL3 staining, and to a slight reduction in the nuclear staining of MBD-R2 and NSL1 compared to the control glands (Figure S5, available online). Depletion of NSL3 protein resulted in a slight reduction in MCRS2 levels, while the staining of NSL1 and MBD-R2 remained unaffected. In contrast, we did not observe any changes in NSL complex members distribution in MBD-R2 and Z4 depleted glands (Figure S5).

The reduction in staining could be a result of impaired stability of the complex caused by degradation of proteins, changes in the transcript levels, and/or changes in nuclear and cytoplasmic distribution of the proteins. In order to address this issue, we used Schneider (SL-2) cells to prepare nuclear and cytoplasmic extracts. The efficiency of nuclear and cytoplasmic extract preparations was measured by detecting tubulin levels, which is enriched in the cytoplasm (Figure 5). The effect of the depletion of MCRS2, MBD-R2, and NSL3 could be reproduced in SL-2 cells using the same RNAi sequences as in the flies (Figures 5A and 5B). Western blot analysis for the components of the NSL complex revealed that in MCRS2 depleted cells, NSL3 and NSL2 protein levels were severely reduced, while MBD-R2 and NSL1 protein levels were slightly affected. These effects were specific to the NSL complex members, as MOF and MSL3 levels remained unchanged (Figure 5A). We observed similar results with NSL1 and NSL3 depletion, where depletion of NSL1 severely affected NSL2 while NSL3 depletion affected the levels of NSL3, NSL1, NSL2, and MBDR2. Levels of other NSL proteins were also moderately compromised in these experiments with the exception of MOF or Tubulin. In contrast, depletion of MOF protein did not affect NSL complex protein levels (Figure 5B).

Furthermore, we found that the NSL complex members are bound to their own genes (Figure S6, available online), suggesting autoregulation by the complex. Consistent with these observations we also noticed a reduction in mRNA levels of NSL2 and NSL3 in MCRS2 depleted cells (Figure S7A, available online). Taken together, these results suggest that the integrity of the NSL complex is interdependent.

Depletion of MCRS2, MBD-R2, and NSL3 Affects the Expression of Target Genes

Polytene chromosome staining as well as the ChIP-Seq approach revealed genome-wide association of NSLs to the promoter regions of a large number of target genes. One of the most obvious questions that arise is whether binding of the NSL complex to target genes is implicated in the regulation of gene expression. *P*-element insertion mutants of MCRS2, MBD-R2, and NSL3 are early larval lethal. So, to measure the effect on transcriptional activity, total RNA was isolated from third instar larval MCRS2, NSL3, and MBD-R2 depleted salivary glands and processed for quantitative reverse transcription (qRT)-PCR analysis (see Experimental Procedures). We chose a set of MCRS2 and NSL1 target genes on both the X chromosome and autosomes to test for a change in transcript levels upon MCRS2, NSL3, and MBD-R2 knockdown. Binding of NSL1, MCRS2, MBD-R2, and MOF to the promoters of these genes was confirmed by ChIP (Figure 3; Figures S2B–S2D). Strikingly, we found a severe reduction in transcript levels for most of the tested NSL complex target genes upon depletion of MCRS2, NSL3, or MBD-R2, respectively (Figures 6B–6D).

Figure 4. ChIP-Seq Analysis Reveals that NSL1 and MCRS2 Bind to Promoters Genome Wide

(A) Snapshot of a chromosome 2R region obtained using Genomatix ElDorado; tracks show read counts for NSL1 and MCRS2 (red). Gene promoters (yellow blocks) and transcripts (gray blocks) are highlighted.

(B) Flybase genes located in the selected region.

(C) Overlap between MCRS2-bound, NSL1-bound, and actively expressed genes in salivary glands.

(D) Chromosomal maps of genes bound by MCRS2 (red) and NSL1 (green). The extent of overlap is shown in yellow. For each chromosome genes on the + strand (top) and − strand (bottom) are shown in gray.

(E) Distribution of fold enrichments for MOF binding, H4K16ac, and H3K27me3 in SL-2 and Kc cells for genes bound (red) and unbound (black) by MCRS2 and NSL1 ($p < 2.2e-16$ in all cases; see Supplemental Experimental Procedures).

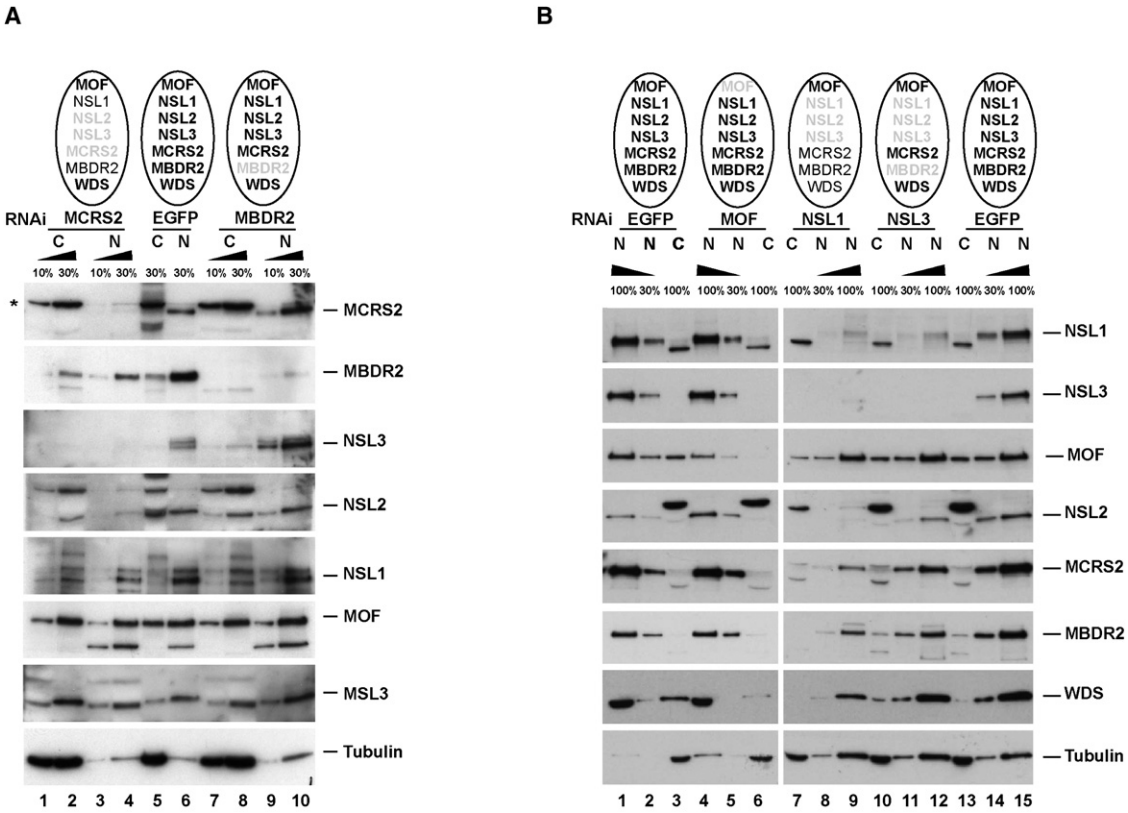

Figure 5. The Stability of the NSL Complex Is Compromised upon Depletion of NSL1, NSL3, and MCRS2

(A) Western blot analysis of the NSL complex members in MCRS2-RNAi, EGFP-RNAi, and MBD-R2-RNAi treated SL-2 cells.

(B) Western blot analysis of the NSL complex members in EGFP-RNAi, MOF-RNAi, NSL1-RNAi, and NSL3-RNAi treated SL-2 cells. C and N are the lanes loaded with cytoplasmic and nuclear extract, respectively. Percentage of extract loaded is also shown. Asterisks indicates the position of a cross-reacting band recognized by MCRS2 in the cytoplasmic fraction. Schematic representation of the NSL protein levels is shown on top of each RNAi condition, where gray color indicates reduced protein levels for the respective protein.

Similar results were obtained when SL-2 cells were depleted of MCRS2 (Figure S7B).

To address whether these effects were also observed on a genome-wide scale we performed gene expression profiling of RNA isolated from MCRS2, MBD-R2, and NSL3 depleted salivary glands using Affymetrix arrays (Figure 6A). We observed that RNAi depletion of any of these proteins results in a very similar pattern of gene expression changes (Figure 6A; Pearson correlation > 0.86 for all comparisons). A total of 5045 genes were differentially expressed in the MCRS2 depleted glands, 3996 genes in the MBD-R2 depleted glands and 4213 genes in the NSL3 depleted glands. In all cases, there was a significant enrichment of differentially expressed genes among the bound ones ($p < 2.2e\text{-}16$ for all three RNAi experiments; Fisher's exact test). Moreover, correlation of genome-wide promoter binding with the expressed genes in the salivary glands revealed 3347 out of 6092 active gene promoters to be bound by both NSL1 and MCRS2 (Figure 4C).

We found similar numbers of up- and downregulated genes among NSL targets, indicating that the loss of the complex is associated with both gene activation and repression. These results were confirmed by qRT-PCR (Figure 6B). A notable exception was MCRS2: The qRT-PCR validation strongly suggested a major activating role. Such a role is difficult to observe using standard array procedures that usually assume a moderated and balanced change on gene expression upon the studied perturbation. To account for this, we performed linear regression between the qRT-PCR and the microarray-generated data (see Supplemental Experimental Procedures). The results indicated a global downregulation upon MCRS2 RNAi depletion that was not observed for any of the other RNAi treatments (data not shown).

Gene expression analysis was also done using salivary glands of male larva that carry the *mof* ^{2} mutation, where a premature stop codon prevents formation of a functional MOF protein (Hilfiker et al., 1997). The effect of NSL depletion on gene expression was generally more severe in its magnitude than the one observed in the absence of MOF (compare Figure 6 with Figure S7C). Furthermore, MCRS2, NSL3, and MBD-R2 depletion did not show a bias for X chromosomal genes, with genes on all chromosomes being similarly affected. Interestingly, binding of the NSL complex members MCRS2, MBD-R2, and NSL1 to chromatin was unaffected in *mof* ^{2} mutant salivary glands as shown by polytene chromosome staining (Figure S8, available

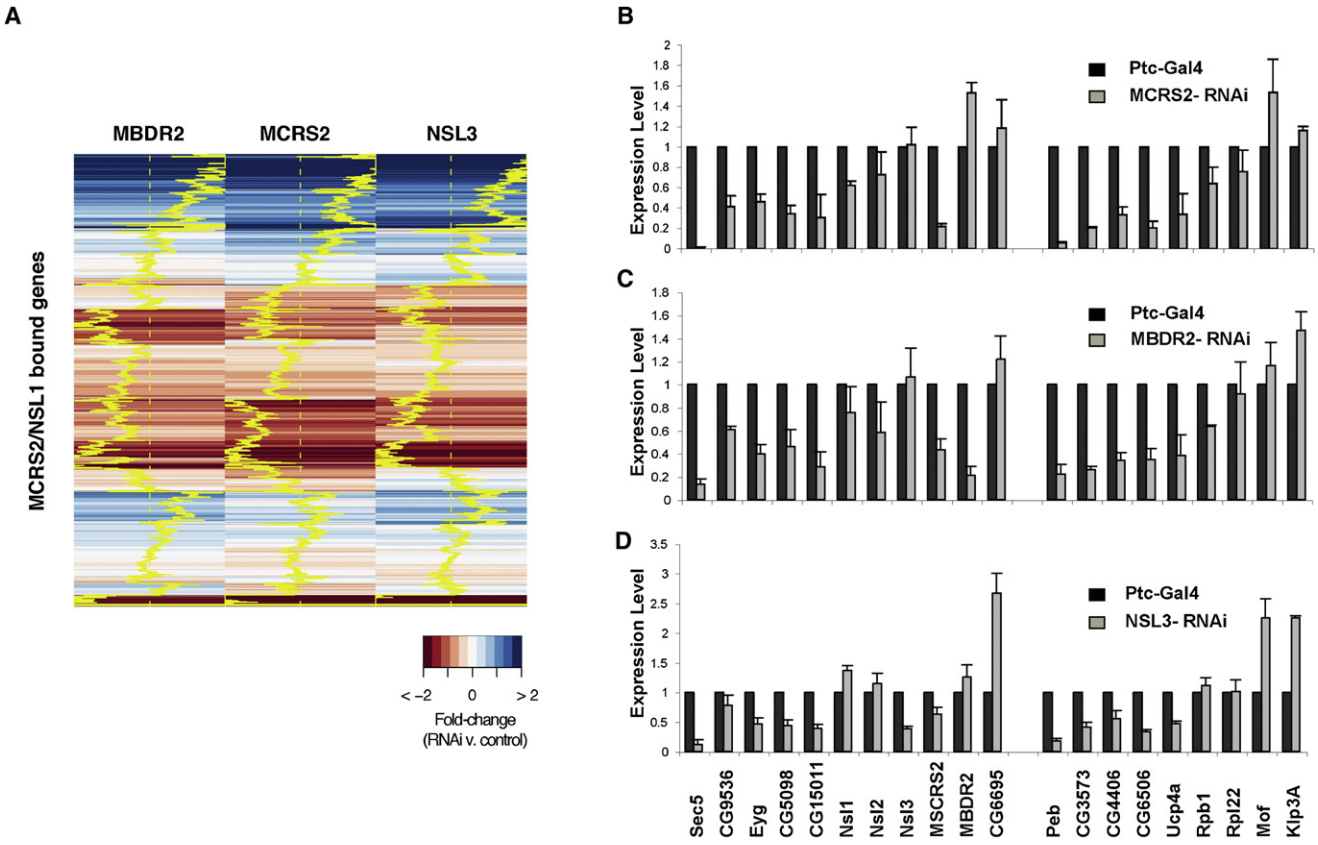

Figure 6. Depletion of MCRS2, MBD-R2, and NSL3 Affects Gene Expression on X Chromosomes and Autosomes

(A) Heatmap displaying gene expression changes upon RNAi depletion of MCRS2, MBDR2, and NSL3 (columns) for genes bound by MCRS2 and NSL1 (rows). Downregulated genes are shown in red. Upregulated genes are shown in blue. Trace lines (yellow) centered in the middle of each column represent the magnitude of the change according to the scale. Both rows and columns were clustered using hierarchical clustering.

(B–D) Quantitative RT-PCR analysis of *Sec5*, *CG9536*, *Eyg*, *CG5098*, *CG15011*, *NSL1*, *NSL2*, *NSL3*, *MCRS2*, *MBD-R2*, and *CG6695* located on autosomes and *Peb*, *CG3573*, *CG4406*, *CG6506*, *Ucp4a*, *Rpb1*, *Rpl22*, *Mof*, and *Klp3A* located on the X chromosome. Wild-type control *Ptc-GAL4* salivary gland expression (black bars) and RNAi depleted salivary gland expression (gray bars). *Ptc-Gal4;UAS-MCRS2-RNAi* (B), *Ptc-Gal4;UAS-MBD-R2-RNAi* (C), and *Ptc-Gal4;UAS-NSL3-RNAi* (D). Error bars represent standard deviation (StDev) of three independent experiments. Expression levels were normalized against the respective genomic DNA.

online). These results suggest a role of NSLs in transcription regulation upstream of MOF function. We therefore propose the evolutionarily conserved NSL complex as an important transcriptional regulator in *Drosophila.*

Depletion of MCRS2 Affects the Integrity of the NSL Complex at Promoters

To further assess whether MCRS2 is required to stably maintain the integrity of the NSL complex on chromatin, we performed ChIP for NSL1, MBD-R2, and MOF on NSL1 and MCRS2 target genes upon MCRS2 depletion. We chose RNAi-mediated knockdown in SL-2 cells, since salivary glands are greatly reduced in size upon MCRS2 knockdown, thus limiting the amount of sample available for ChIP. As expected, depletion of MCRS2 led to reduced levels of MCRS2 at target promoters (Figure 7A) and up to 90% of knockdown efficiency (Figure 5A). Interestingly, depletion of MCRS2 resulted in a severe reduction in the binding of NSL1 and MBD-R2 to these target genes (Figure 7A), while their overall protein levels were only moderately affected (Figure 5). These results demonstrate that MCRS2 is required to stably maintain the integrity of the NSL complex at target promoters.

Furthermore, although the protein level of MOF was unaffected upon depletion of MCRS2 (Figure 5A), MOF binding to target promoters was substantially reduced (Figure 7A). Similar results were obtained by performing ChIP on whole larvae using an MCRS2 mutant (Figures S9A–S9C, available online). We also tested the effects of MCRS2 depletion on the levels of H4K16Ac and H3K4me3, as both marks are associated with active genes. ChIP using antibody against histone H4 was used as control. We observed no significant reduction in H3K4me3 levels at these promoters, however, acetylation at H4K16 was moderately reduced upon depletion of MCRS2 (Figure 7A). Moderate reduction of H4K16Ac may be explained by the dynamic nature of MOF interaction at these sites or a low H4K16Ac turnover. However, another very likely possibility could be that since these

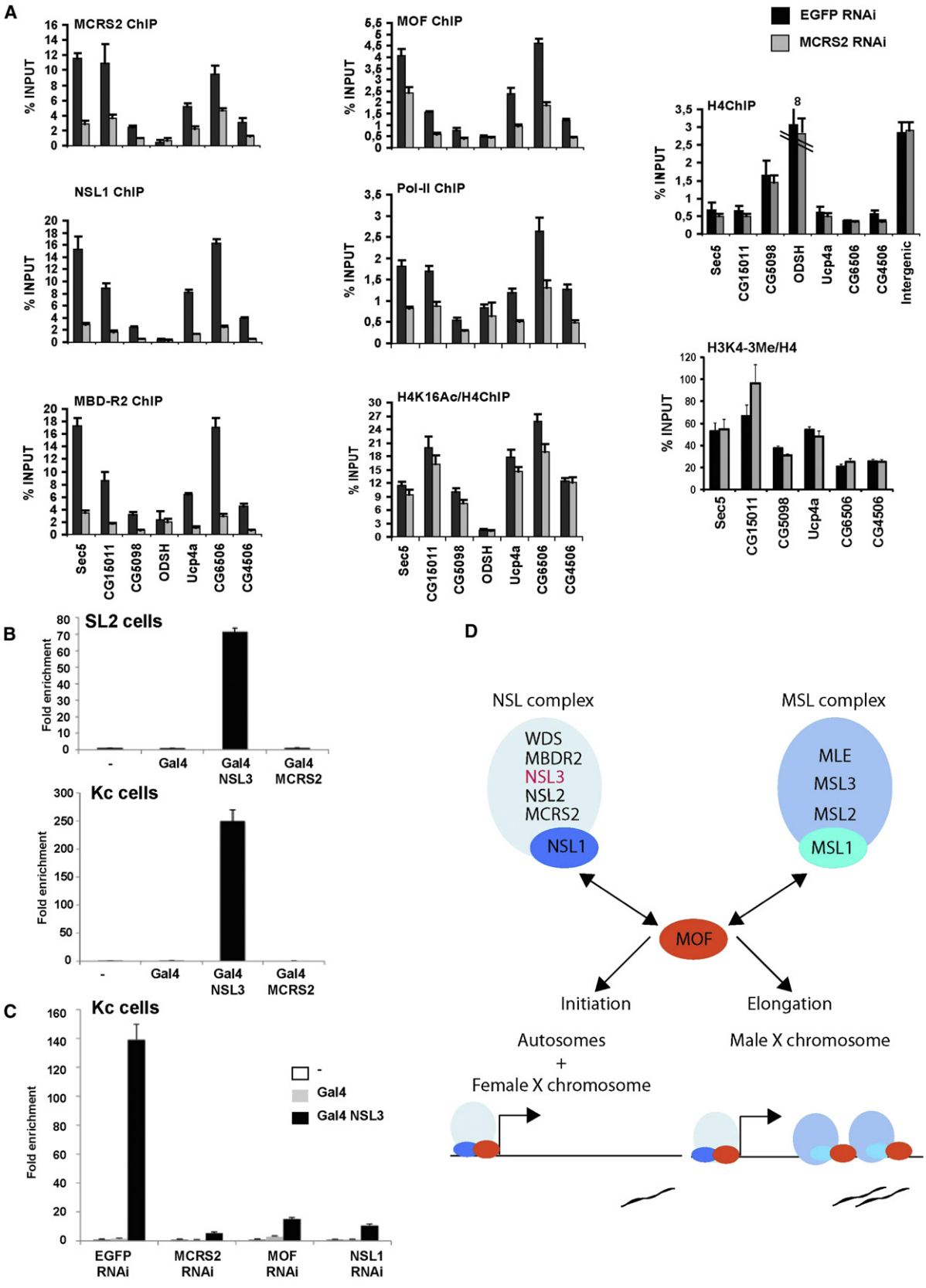
A
MCRS2 ChIP
MOF ChIP
EGFP RNAi
MCRS2 RNAi
NSL1 ChIP
Pol-II ChIP
H4ChIP
MBD-R2 ChIP
H4K16Ac/H4ChIP
H3K4-3Me/H4
% INPUT
Sec5
CG15011
CG5098
ODSH
Ucp4a
CG6506
CG4506
Intergenic
B
SL2 cells
Kc cells
Fold enrichment
-
Gal4
Gal4 NSL3
Gal4 MCRS2
C
Kc cells
Gal4
Gal4 NSL3
EGFP RNAi
MCRS2 RNAi
MOF RNAi
NSL1 RNAi
D
NSL complex
MSL complex
WDS
MBDR2
NSL3
NSL2
MCRS2
NSL1
MLE
MSL3
MSL2
MSL1
MOF
Initiation
Elongation
Autosomes
+
Female X chromosome
Male X chromosome

ChIPs were performed in SL-2 cells, presence of the MSL complex may still be responsible for overall acetylation levels. Indeed, when comparing MOF levels at the 5′ versus 3′ end of X-linked genes, we observed a more significant reduction at the promoters versus the 3′ end upon MCRS2 depletion (Figure S9D). Consistent with these observations, when we repeated the ChIP in Kc cells depleted of MCRS2, where the MSL complex is not assembled, NSL1, MBD-R2, and MOF as well as H4K16 levels were severely affected (Figure S10A, available online).

As mentioned earlier, upon depletion of MCRS2, MBD-R2, and NSL3, the mRNA levels of most of the tested target genes were reduced. We were next interested to know whether the reduction in expression of these target genes is a result of defects in the recruitment of RNA polymerase II to their promoters. Depletion of MCRS2 led to a severe loss of NSL1, NSL2, NSL3, and MBD-R2 from gene promoters. We therefore chose to assay the binding of RPB3—a subunit of the core RNA polymerase II (Adelman et al., 2005) on the target genes in MCRS2 depleted cells. Interestingly, the levels of RPB3 on target promoters were significantly reduced in MCRS2 depleted cells (Figure 7A). However, overall nuclear RNA polymerase II levels remain unaffected as shown by western blot (Figure S10B). These results suggest that the reduction in expression upon loss of the NSL complex from its target genes might be a consequence of altered recruitment of RNA polymerase II to the promoters, suggesting a function of NSLs in early transcriptional regulation.

NSL3-Driven Transcription Activation Is Modulated by NSL1, MCRS2, and MOF

Next, we were interested in studying whether the NSL complex has the potential to activate transcription. We therefore expressed two components of the NSL complex, NSL3 and MCRS2, fused to the Gal4 DNA-binding domain in SL-2 or Kc cells cotransfected with a UAS-driven luciferase reporter. Interestingly, expression of Gal4-NSL3 resulted in potent activation of the reporter (Figure 7B). In contrast, transfection of Gal4 alone or Gal4-MCRS2 did not show activation of the reporter gene. We next tested whether activation by Gal4-NSL3 is sensitive to the endogenous levels of NSL complex members. For this purpose we depleted NSL1 and MCRS2 as well as MOF in cells transfected with Gal4-NSL3 or Gal4-DBD as a control. Reduction in levels of NSL1 or MCRS2 severely affected the transcription activation mediated by NSL3. Similarly, depletion of MOF substantially reduced reporter activation (Figure 7C). These results strongly suggest that the NSL complex members and MOF work synergistically to activate transcription.

DISCUSSION

Here we report the biochemical purification and functional analysis of the NSL complex. The members of this complex are evolutionarily conserved between fruit flies and humans (Mendjan et al., 2006). Intriguingly, we find that 55% of all active genes are bound by the NSL complex in *Drosophila*. We show that loss of binding of these factors severely affects expression of target genes. Interestingly, loss of NSL proteins affects MOF binding as well as RNA pol II recruitment to promoters. Furthermore, we show that the NSL complex and MOF work synergistically to activate transcription. Taken together, these results identify the NSL complex as a transcriptional regulator in the *Drosophila* genome.

Genome-wide Colocalization of the NSL Complex Members on Gene Promoters

We present several lines of evidence that the NSL complex resides at gene promoters. First, immunostaining of polytene chromosomes with antibodies against NSL complex members and MOF highly colocalizes in both sexes (Figure 2; Figure S2A). Second, NSL1, MCRS2, MBD-R2, and MOF colocalize at the promoters of the tested MOF target genes in salivary glands as shown by ChIP experiments (Figure 3). The NSL complex binding at promoters is not restricted to salivary glands, as we found essentially the same results using chromatin from SL-2 cells and whole larvae (Figures S2B–S2D). Finally, using ChIP and Solexa sequencing, we show that NSL1 and MCRS2 signals highly overlap at the promoters of ~4000 genes in salivary glands (Figure 4). There is a striking correlation between promoter-bound NSL complex members and MOF as over 70% of previously identified MOF-bound promoters in SL-2 and Kc cells (Kind et al., 2008) overlap with promoter-bound NSL1 and MCRS2 in male salivary glands (Figure 4E).

Figure 7. Depletion of MCRS2 Affects the Integrity of the NSL Complex at Target Promoters

(A) ChIP using antibodies against MCRS2, NSL1, MBD-R2, MOF, Rpb3 (Pol II), Histone H4, and H4K16Ac on four X-linked genes (*OdsH*, *Ucp4A*, *CG6506*, and *CG4406*) and three autosomal genes (*Sec5*, *CG15011*, and *CG5098*) in EGFP-RNAi treated (black bars) and MCRS2-RNAi treated (gray bars) SL-2 cells. Primers were positioned at the promoters of the mentioned genes. Exact positions of the primers are described in the Supplemental Data. Percentage input is determined as the amount of immunoprecipitated DNA relative to input DNA. Error bars represent standard deviation (StDev) of four independent experiments.

(B) Tethering NSL3 via the GAL4 DNA-binding domain activates transcription of the luciferase reporter under the UAS promoter in SL-2 cells (top) and Kc cells (bottom). Transient transfection of either empty vector (–), vector expressing the GAL4 DNA-binding domain (Gal4), GAL4NSL1, GAL4NSL3, or GAL4MCRS2. Error bars represent standard deviation (StDev) of three independent experiments.

(C) NSL3-mediated transcription activation is affected by depletion of MCRS2, NSL1, and MOF. Transient transfection of either empty vector (–), vector expressing GAL4 DNA-binding domain (Gal4), or GAL4NSL3 in cells treated with EGFP RNAi, MCRS2 RNAi, MOF RNAi, or NSL1 RNAi. *y* axis shows fold enrichment compared to vector control. Error bars represent standard deviation (StDev) of three independent experiments.

(D) Summary model: MOF protein is present in two distinct complexes. The classical MSL complex (or the dosage compensation complex) that is enriched on the 3′ end of X-linked genes and the NSL complex that is a promoter-bound complex. Within these two complexes MOF directly interacts with either MSL1 or NSL1, two PEHE domain-containing proteins. The stability of the NSL complex is interdependent, MCRS2, NSL1, and NSL3 playing a major role in the overall stability of the complex. Tethering NSL3 via Gal4 DNA-binding domain to a UAS containing heterologous reporter activates transcription in both SL-2 and Kc cells and this activation is modulated by the presence of NSL1, MCRS2, or MOF. We propose a working model that synergistic interaction of the NSL complex with MOF at promoters might promote transcription initiation, while interaction of MOF with the MSL complex at the 3′ end of X-linked genes may facilitate transcription elongation.

It was previously shown that depletion of MSL1 led to the loss of MOF from the 3′ end of X-linked target genes in males, but, surprisingly, MOF binding at the promoters of the same genes was unaffected (Kind et al., 2008). The results shown in the present study unravel that MOF binds to the promoters in an association with the NSL complex and that this association is not restricted to the male X chromosome, but is genome wide in both sexes. The observation that MOF binding at promoters is reduced upon depletion of MCSR2 clearly suggests that the NSL complex contributes to the recruitment of MOF to target gene promoters (Figure 7). However, chromatin binding of the NSL complex members is not affected in the absence of MOF, implicating NSLs in transcription regulation upstream of MOF. These data reveal a hierarchy of recruitment at these target promoters. Furthermore, it is noteworthy that NSL mutants are early larval lethal in both sexes, whereas, Mof mutants are male lethal due to dosage compensation defects, but females are viable to the adult stage albeit being sterile (Gelbart et al., 2009). These observations suggest that NSL1, NSL2, NSL3, MCRS2, and MBD-R2 are important regulators during fly development and play additional functions very likely independent of MOF.

MCRS2 Is Required to Stably Maintain the NSL Complex on Promoters

We find that the integrity of the NSL complex is interdependent, very likely operating at both transcriptional and posttranscriptional levels. Our study identifies NSL1 and MCRS2 among the key players in maintaining the integrity of the NSL complex. Depletion of MCRS2 not only affected protein levels of NSL2 and NSL3, but ChIP analysis also revealed that in the absence of MCRS2, the rest of the complex is unable to achieve efficient chromatin targeting. There is an interesting resemblance of the above observations with that of the MSL complex where the MSL2 protein is required for complex stability (Beckmann et al., 2005; Gebauer et al., 2003; Grskovic et al., 2003; Kelley et al., 1997).

MCRS2 contains a FHA domain at its C terminus. The FHA domain is a phosphopeptide recognition domain found in many regulatory proteins. It displays specificity for phosphothreonine-containing epitopes but also recognizes phosphotyrosine with relatively high affinity (Durocher and Jackson, 2002). It is provocative to speculate that MCRS2 could recognize the phosphorylated forms of the members of the NSL complex through the FHA domain to stabilize and recruit the complex to its target promoters.

The NSL Complex Regulates Transcription at Promoters

Depletion of NSL components resulted in expression changes of many of the NSL-bound genes on autosomes as well as on the X chromosome. Importantly, magnitude and extent of the expression effect was more severe than the one observed in the absence of MOF, suggesting a MOF-independent mechanism for NSL function. However, it remains possible that the role of MOF at target promoters is to fine tune gene expression by modulating NSL function. This is further supported by our observations that NSL3-mediated transcription activation is sensitive to endogenous MOF levels. The broad polytene chromosome staining as well as ChIP-Seq analysis of the NSLs shows that many chromatin regions are occupied by the NSL complex, which is likely to be involved in the regulation of a wide spectrum of genes (Figure 7D).

The observation that RNA polymerase II recruitment to target genes is affected upon depletion of MCRS2 suggests that the NSL complex is involved in early steps of transcription. Taking into account that over 4000 promoters are bound by both NSL1 and MCRS2, correlating with ~55% of the active genes, and that the expression of most of the NSL target genes tested in this study is compromised upon the loss of NSL complex members in salivary glands, several fundamental questions emerge: How is the NSL complex targeted to responsive promoters? Which step of transcription initiation requires the presence of the NSL complex?

The NSL complex could possibly recognize specific DNA sequences at promoter regions or is brought to promoters through the interactions with components of the transcription machinery or regulatory proteins present on the promoters. These interactions would most probably be transient, and reflect an inherent instability, as no such proteins were found purifying with the NSL complex members.

Another very likely possibility is that the complex recognizes histone marks. The NSL proteins harbor a rich composition of chromatin-binding domains. For example, WDS is a protein with the potential of binding to histone H3. It belongs to the WD family and consists of seven WD40 repeats (Hollmann et al., 2002). It is known that these repeats are involved in protein-protein interaction and are present in many chromatin-associated complexes (Cao et al., 2002). The mammalian ortholog of this protein, WDR5, binds specifically to the N-terminal tail of histone H3 and thereby helps to recruit the MLL containing H3K4-specific methyltransferase complex to its target promoters (Wysocka et al., 2005). Methylated H3K4 is coupled to transcription activation (Zhang and Reinberg, 2001). We show that H3K4me3 is unaffected in the absence of MCRS2, indicating that the NSL complex recruitment could be downstream of this activation mark. WDS could potentially have analogous functions in recruiting the NSL complex to target promoters in order to regulate the transcription of target genes. Another member of the complex is MBD-R2, which has a Tudor and methyl binding (MBD) domains (Taipale et al., 2005). Tudor domains share similarity to chromodomains, which also bind methylated residues (Lachner et al., 2001). In yeast, Tudor domains have been shown to bind methylated H3K79 (Huyen et al., 2004). MBD domains bind to methylated DNA and are involved in transcriptional repression in mammals (Bird, 2002). However, DNA methylation happens much more seldom in *Drosophila* than in mammals and its function remains unclear (Lyko et al., 2000). MBD-R2 is therefore another candidate that could recognize modified histones and target the NSL complex to promoters in *Drosophila*.

It is important to emphasize that we have shown earlier that the mammalian orthologs of the *Drosophila* NSL complex members were found copurifying with human MOF (Mendjan et al., 2006). These observations have been further confirmed recently (Cai et al., 2010). The mammalian NSL complex was shown to have a more relaxed substrate specificity acetylating histone H4 lysine 5, 8, and 16, in comparison to the MSL complex where MOF

preferentially acetylates histone H4 lysine 16 (Cai et al., 2010; Mendjan et al., 2006). Similar to the *Drosophila* MOF protein which can acetylate nonhistone substrates (Buscaino et al., 2003; Morales et al., 2004), mammalian MOF alone or in association with MSL1v1 (NSL1) has recently been shown to acetylate other nonhistone substrates such as TIP5 or p53, respectively (Li et al., 2009; Zhou et al., 2009). It therefore remains to be seen in the future whether the mammalian NSL complex could also play a more global role in transcriptional regulation. Besides transcription, NSL components have also recently been implicated in other cellular processes (Dobbelaere et al., 2008; Nybakken et al., 2005). In summary, the biochemical purification and functional characterization of NSL proteins described in this study reveals an important evolutionarily conserved genome-wide promoter-bound complex that acts as a major transcriptional regulator in *Drosophila*.

EXPERIMENTAL PROCEDURES

Biochemical Purifications

Biochemical purifications from SL-2 cells expressing tagged proteins (TAP-MCRS2 or HA/FLAG NSL1) were always accompanied with control purifications from wild-type SL-2 nuclear extract to be able to compare specific enrichment.

TAP purifications were done essentially as described (Rigaut et al., 1999) with the following changes in the protocol: All buffers contained 25 mM HEPES (pH 7.6) instead of Tris-HCL, KCl instead of NaCl, 1/100 volume of RNasin (Promega), 0.2% Tween-20, and 20% glycerol. For details on HA/FLAG purifications see Supplemental Experimental Procedures.

Silver Staining and Mass Spectrometry

Silver staining and mass spectrometry were performed as previously described (Shevchenko et al., 1996). Purified protein samples were prepared for mass spectrometry in two ways. Either individual silver-stained protein bands were digested in gel with trypsin (Figure 1A) or complex elutions were electrophoresed for a few minutes, nonseparated proteins stained with Coomassie blue, total band excised, and trypsin digested (Table S1). The samples were separated for 45 min on a nano-flow 1D-plus Eksigent (Eksigent, Dublin, CA) HPLC system coupled to a qStar Pulsar i quadrupole time-of-flight mass spectrometer (Applied Biosystems, Darmstadt, Germany). Analysis was performed as described (Fraterman et al., 2007). Taxonomy parameter was restricted to *Drosophila*, and peptides below a score of 18 were excluded. All proteins were identified with a summed peptide MASCOT score above 45 in at least two independent experiments.

Biochemical Interaction Assays

Recombinant full-length NSL1, MCRS2, and MOF were either singularly or coexpressed using the baculovirus coexpression system. Details of the purification are available upon request.

For the hMOF/NSL1 interaction, a His-tag fusion of the C-terminal fragment of hNSL1 (883–1105) and untagged MOF HAT domain (174–458) were coexpressed in *E. coli* BL21Star(DE3) (Invitrogen) from pProEXHTb (Invitrogen) and pRSFDuet-1 (Novagen) expression vectors, respectively. The complex was first purified by affinity chromatography using Ni^{2+} resin. In parallel, a His-tag version of hMOF(174–458) was expressed from pProEXHTb. The His tag was removed by TEV protease following the Ni^{2+} affinity chromatography. The gel-filtration profiles were obtained using Superdex 200 column (GE Healthcare).

RNAi in SL-2 Cells, Nuclear, and Cytoplasmic Fractions

RNAi of SL-2 and Kc cells was performed as described in Worby et al. (2001) with the following modifications. All knockdown cells were transfected with 50 μg dsRNA using Lipofectamine (Invitrogen). The cells were harvested after 6 days for MCRS2 RNAi. EGFP control RNAi experiments were performed in parallel. Nuclear and cytoplasmic extracts were done from 2×10^6 cells. The cell pellet was dissolved in HEMG 40 (HEMG buffer contains 25 mM HEPES pH 7.6, 0.5 mM EDTA, 5 mM MgCl2, and 20% glycerol; so HEMG 40 is HEMG with 40 mM KCl), and placed for 10 min on ice for swelling. NP40 was added to 1% final concentration, vortexed for 7 s, and centrifuged at 3000 rpm for 5 min. The supernatant containing cytoplasmic extract was carefully removed to a new eppendorf tube and 4× Laemmli buffer was added. The nuclei pellet was washed extensively with HEMG 150 and lysed in 2× Laemmli buffer.

RNAi Knockdown in Larval Salivary Glands

The homozygous transgenic RNAi fly strains carrying *UAS-MCRS2-RNAi*, *UAS-NSL3-RNAi*, *UAS-MBD-R2-RNAi*, and *UAS-Z4-RNAi* were independently crossed to *Ptc-Gal4*, *UAS-eGFP*, and raised at 25°C to obtain efficient knockdown. Salivary glands from third instar larvae were dissected in PBS and processed for either immunofluroscence antibody staining or for RNA isolation and qRT-PCR analysis. Antibodies against NSL1, NSL3, MCRS2, MBD-R2, MOF, H4K16Ac, MSL1, and Z4 for IF were used at 1:100 dilution.

RNA Isolation and Quantitative PCR Analysis

For qRT-PCR, RNA and corresponding genomic DNA from SL-2 cells or from salivary glands were isolated simultaneously using the AllPrep DNA/RNA mini kit (QIAGEN), the RNA column was DNaseI treated, and 300 ng of total RNA was used in a RT reaction. qRT-PCR was performed on a Applied Biosystems (AP) Cycler7500 with SYBR detection, and the amplification curves were analyzed with the corresponding AP software. Each qRT-PCR was repeated at least three times, values were normalized to corresponding genomic DNA values, and the standard deviation within each experiment was calculated.

qPCR analysis of the ChIP samples was performed using the SYBR Green PCR master mix (Applied Biosystem), 100 ng of each forward and reverse primer, and 1 μl immunoprecipitated DNA, in an ABI7500 real-time PCR thermocycler (Applied Biosystems, Inc.). The formula [%ChIP/input] = $[E^{(Ct_{input} - Ct_{ChIP})} \times 100\%]$ (E represents primer annealing efficiency) was used to calculate the percentage of DNA recovery after ChIP, as compared to the amount of input material. The primers designed for the promoter (P1), middle (P2) and the end (P3) of the gene were used for the binding analysis.

Immunofluorescence and Confocal Microscopy

Preparation of polytene chromosomes was performed as described (http://www.igh.cnrs.fr/equip/cavalli/Lab%20Protocols/Immunostaining.pdf). MOF and MSL1 antibodies were used at 1:500 dilution, MBD-R2 at 1:300, and MCRS2 and NSL1 at 1:50. Immunofluorescence stainings of whole-mount salivary glands were essentially done as described (Beuchle et al., 2001). Images were captured with AxioCamHR CCD camera on a Leica SP5 (Leica Microsystems) using an Apochromat NA 1.32 oil immersion objective. Images were arranged with Adobe Illustrator.

ACCESSION NUMBERS

Microarray expression data are available in the ArrayExpress database under accession number E-MEXP-2652, and the ChIP-seq data are available under accession number E-MTAB-214.

SUPPLEMENTAL INFORMATION

Supplemental Information includes Supplemental Experimental Procedures, 10 figures, and 2 tables and can be found with this article online at doi:10.1016/j.molcel.2010.05.021.

ACKNOWLEDGMENTS

We are grateful to the members of the lab for useful discussions and critical reading of the manuscript. We thank Nic Tapon and Ditte Anderson for communication of results prior to publication. We thank Matthias Wilm and Marc Gentzel for support for mass spectrometry analysis. We thank Vladimir Benes, Tomi Baehr-Ivacevic, and Johanthan Blake in the Genomics core

facility for processing of the ChIP-sequencing samples. We thank John T. Lis for providing us the anti-RPB3 antibody. We are grateful to Stephen Cusack for support. We thank Marc Jamin for help with the MALLS experiment. We thank Erinc Hallacli and Ibrahim Ilik for critical reading of the manuscript. This work was funded from Deutsche Forschungsgemeinschaft-Sonderforschungsbereiche (Transregio) grant and Epigenome Network of Excellence under EU Framework Programme 6 to A.A. P.G. was supported by an "E-STAR" fellowship funded by the EU's FP6 Marie Curie Host fellowship for Early Stage Research Training under contract number MEST-CT-2004-504640.

Received: September 2, 2009
Revised: January 27, 2010
Accepted: April 6, 2010
Published: June 24, 2010

REFERENCES

Adelman, K., Marr, M.T., Werner, J., Saunders, A., Ni, Z., Andrulis, E.D., and Lis, J.T. (2005). Efficient release from promoter-proximal stall sites requires transcript cleavage factor TFIIS. Mol. Cell *17*, 103–112.

Akhtar, A., and Becker, P.B. (2000). Activation of transcription through histone H4 acetylation by MOF, an acetyl transferase essential for dosage compensation in Drosophila. Mol. Cell *5*, 367–375.

Alekseyenko, A.A., Larschan, E., Lai, W.R., Park, P.J., and Kuroda, M.I. (2006). High-resolution ChIP-chip analysis reveals that the Drosophila MSL complex selectively identifies active genes on the male X chromosome. Genes Dev. *20*, 848–857.

Alekseyenko, A.A., Peng, S., Larschan, E., Gorchakov, A.A., Lee, O.K., Kharchenko, P., McGrath, S.D., Wang, C.I., Mardis, E.R., Park, P.J., et al. (2008). A sequence motif within chromatin entry sites directs MSL establishment on the Drosophila X chromosome. Cell *134*, 599–609.

Beckmann, K., Grskovic, M., Gebauer, F., and Hentze, M.W. (2005). A dual inhibitory mechanism restricts msl-2 mRNA translation for dosage compensation in Drosophila. Cell *122*, 529–540.

Beuchle, D., Struhl, G., and Muller, J. (2001). Polycomb group proteins and heritable silencing of Drosophila Hox genes. Development *128*, 993–1004.

Bird, A. (2002). DNA methylation patterns and epigenetic memory. Genes Dev. *16*, 6–21.

Brand, A.H., and Perrimon, N. (1993). Targeted gene expression as a means of altering cell fates and generating dominant phenotypes. Development *118*, 401–415.

Buscaino, A., Kocher, T., Kind, J.H., Holz, H., Taipale, M., Wagner, K., Wilm, M., and Akhtar, A. (2003). MOF-regulated acetylation of MSL-3 in the Drosophila dosage compensation complex. Mol. Cell *11*, 1265–1277.

Cai, Y., Jin, J., Swanson, S.K., Cole, M.D., Choi, S.H., Florens, L., Washburn, M.P., Conaway, J.W., and Conaway, R.C. (2010). Subunit composition and substrate specificity of a MOF-containing histone acetyltransferase distinct from the male-specific lethal (MSL) complex. J. Biol. Chem. *285*, 4268–4272.

Cao, R., Wang, L., Wang, H., Xia, L., Erdjument-Bromage, H., Tempst, P., Jones, R.S., and Zhang, Y. (2002). Role of histone H3 lysine 27 methylation in Polycomb-group silencing. Science *298*, 1039–1043.

Dobbelaere, J., Josue, F., Suijkerbuijk, S., Baum, B., Tapon, N., and Raff, J. (2008). A genome-wide RNAi screen to dissect centriole duplication and centrosome maturation in Drosophila. PLoS Biol. *6*, e224.

Durocher, D., and Jackson, S.P. (2002). The FHA domain. FEBS Lett. *513*, 58–66.

Fraterman, S., Zeiger, U., Khurana, T.S., Wilm, M., and Rubinstein, N.A. (2007). Quantitative proteomics profiling of sarcomere associated proteins in limb and extraocular muscle allotypes. Mol. Cell. Proteomics *6*, 728–737.

Gebauer, F., Grskovic, M., and Hentze, M.W. (2003). Drosophila sex-lethal inhibits the stable association of the 40S ribosomal subunit with msl-2 mRNA. Mol. Cell *11*, 1397–1404.

Gelbart, M.E., Larschan, E., Peng, S., Park, P.J., and Kuroda, M.I. (2009). Drosophila MSL complex globally acetylates H4K16 on the male X chromosome for dosage compensation. Nat. Struct. Mol. Biol. *16*, 825–832.

Gilfillan, G.D., Straub, T., de Wit, E., Greil, F., Lamm, R., van Steensel, B., and Becker, P.B. (2006). Chromosome-wide gene-specific targeting of the Drosophila dosage compensation complex. Genes Dev. *20*, 858–870.

Grskovic, M., Hentze, M.W., and Gebauer, F. (2003). A co-repressor assembly nucleated by Sex-lethal in the 3′UTR mediates translational control of Drosophila msl-2 mRNA. EMBO J. *22*, 5571–5581.

Hendrich, B., and Tweedie, S. (2003). The methyl-CpG binding domain and the evolving role of DNA methylation in animals. Trends Genet. *19*, 269–277.

Hilfiker, A., Hilfiker-Kleiner, D., Pannuti, A., and Lucchesi, J.C. (1997). mof, a putative acetyl transferase gene related to the Tip60 and MOZ human genes and to the SAS genes of yeast, is required for dosage compensation in Drosophila. EMBO J. *16*, 2054–2060.

Hollmann, M., Simmerl, E., Schafer, U., and Schafer, M.A. (2002). The essential Drosophila melanogaster gene wds (will die slowly) codes for a WD-repeat protein with seven repeats. Mol. Genet. Genomics *268*, 425–433.

Huyen, Y., Zgheib, O., Ditullio, R.A., Jr., Gorgoulis, V.G., Zacharatos, P., Petty, T.J., Sheston, E.A., Mellert, H.S., Stavridi, E.S., and Halazonetis, T.D. (2004). Methylated lysine 79 of histone H3 targets 53BP1 to DNA double-strand breaks. Nature *432*, 406–411.

Kelley, R.L., Wang, J., Bell, L., and Kuroda, M.I. (1997). Sex lethal controls dosage compensation in Drosophila by a non-splicing mechanism. Nature *387*, 195–199.

Kind, J., Vaquerizas, J.M., Gebhardt, P., Gentzel, M., Luscombe, N.M., Bertone, P., and Akhtar, A. (2008). Genome-wide analysis reveals MOF as a key regulator of dosage compensation and gene expression in Drosophila. Cell *133*, 813–828.

Kouzarides, T. (2007). Chromatin modifications and their function. Cell *128*, 693–705.

Lachner, M., O'Carroll, D., Rea, S., Mechtler, K., and Jenuwein, T. (2001). Methylation of histone H3 lysine 9 creates a binding site for HP1 proteins. Nature *410*, 116–120.

Legube, G., McWeeney, S.K., Lercher, M.J., and Akhtar, A. (2006). X-chromosome-wide profiling of MSL-1 distribution and dosage compensation in Drosophila. Genes Dev. *20*, 871–883.

Lemon, B., and Tjian, R. (2000). Orchestrated response: a symphony of transcription factors for gene control. Genes Dev. *14*, 2551–2569.

Li, X., Wu, L., Corsa, C.A., Kunkel, S., and Dou, Y. (2009). Two mammalian MOF complexes regulate transcription activation by distinct mechanisms. Mol. Cell *36*, 290–301.

Lyko, F., Ramsahoye, B.H., and Jaenisch, R. (2000). DNA methylation in Drosophila melanogaster. Nature *408*, 538–540.

Mendjan, S., Taipale, M., Kind, J., Holz, H., Gebhardt, P., Schelder, M., Vermeulen, M., Buscaino, A., Duncan, K., Mueller, J., et al. (2006). Nuclear pore components are involved in the transcriptional regulation of dosage compensation in Drosophila. Mol. Cell *21*, 811–823.

Morales, V., Straub, T., Neumann, M.F., Mengus, G., Akhtar, A., and Becker, P.B. (2004). Functional integration of the histone acetyltransferase MOF into the dosage compensation complex. EMBO J. *23*, 2258–2268.

Nybakken, K., Vokes, S.A., Lin, T.Y., McMahon, A.P., and Perrimon, N. (2005). A genome-wide RNA interference screen in Drosophila melanogaster cells for new components of the Hh signaling pathway. Nat. Genet. *37*, 1323–1332.

Orphanides, G., and Reinberg, D. (2000). RNA polymerase II elongation through chromatin. Nature *407*, 471–475.

Rigaut, G., Shevchenko, A., Rutz, B., Wilm, M., Mann, M., and Seraphin, B. (1999). A generic protein purification method for protein complex characterization and proteome exploration. Nat. Biotechnol. *17*, 1030–1032.

Schwartz, Y.B., Kahn, T.G., Nix, D.A., Li, X.Y., Bourgon, R., Biggin, M., and Pirrotta, V. (2006). Genome-wide analysis of Polycomb targets in Drosophila melanogaster. Nat. Genet. *38*, 700–705.

Shevchenko, A., Wilm, M., Vorm, O., and Mann, M. (1996). Mass spectrometric sequencing of proteins silver-stained polyacrylamide gels. Anal. Chem. *68*, 850–858.

Smith, E.R., Pannuti, A., Gu, W., Steurnagel, A., Cook, R.G., Allis, C.D., and Lucchesi, J.C. (2000). The drosophila MSL complex acetylates histone H4 at lysine 16, a chromatin modification linked to dosage compensation. Mol. Cell. Biol. *20*, 312–318.

Smith, E.R., Allis, C.D., and Lucchesi, J.C. (2001). Linking global histone acetylation to the transcription enhancement of X-chromosomal genes in Drosophila males. J. Biol. Chem. *276*, 31483–31486.

Taipale, M., Rea, S., Richter, K., Vilar, A., Lichter, P., Imhof, A., and Akhtar, A. (2005). hMOF histone acetyltransferase is required for histone H4 lysine 16 acetylation in mammalian cells. Mol. Cell. Biol. *25*, 6798–6810.

Thomas, M.C., and Chiang, C.M. (2006). The general transcription machinery and general cofactors. Crit. Rev. Biochem. Mol. Biol. *41*, 105–178.

Worby, C., Simonson-Leff, N., and Dixon, J.E. (2001). RNA interference of gene expression (RNAi) in cultured Drosophila cells. Sci. STKE *95*, pl1.

Wysocka, J., Swigut, T., Milne, T.A., Dou, Y., Zhang, X., Burlingame, A.L., Roeder, R.G., Brivanlou, A.H., and Allis, C.D. (2005). WDR5 associates with histone H3 methylated at K4 and is essential for H3 K4 methylation and vertebrate development. Cell *121*, 859–872.

Zhang, Y., and Reinberg, D. (2001). Transcription regulation by histone methylation: interplay between different covalent modifications of the core histone tails. Genes Dev. *15*, 2343–2360.

Zhou, Y., Schmitz, K.M., Mayer, C., Yuan, X., Akhtar, A., and Grummt, I. (2009). Reversible acetylation of the chromatin remodelling complex NoRC is required for non-coding RNA-dependent silencing. Nat. Cell Biol. *11*, 1010–1016.